Effects of the Plasma Conductivity on Transverse Instabilities in High-Intensity Ion Beam

Han S. Uhm and Ronald C. Davidson

***Abstract*—A stability analysis of a propagating ion beam through a plasma medium is carried out in terms of transverse conductivity of the background plasma. Coupled eigenvalue equations are obtained for the flat-top density profiles of beam ions and plasma electrons. The dispersion relation of the transverse instability in an intense ion beam propagating through the background plasma is derived, including the plasma conductivity $(4\pi\sigma_\perp/\omega)$, the magnetic decay time τ_d and fractional charge neutralization f. It is shown that the obtained dispersion relation recovers the previous one of the electron-ion two-stream instability in the limit of $\sigma_\perp \rightarrow 0$. On the other hand, the dispersion relation of the resistive-hose instability is recovered when $\sigma_\perp \rightarrow \infty$. Influence of the finite transverse conductivity $\sigma_\perp$ on the resistive hose stability properties are investigated for the ion beam propagating through a plasma channel. The growth rate of the resistive hose instability decreases considerably as the transverse conductivity $4\pi\sigma_\perp/\omega$ decreases from infinity.**

***Index Terms*—Instability, ion beam, plasma conductivity, resistive-hose, two-stream.**

I. Introduction

HIGH-ENERGY ion accelerators and transportation system [1]–[4] have a wide range of applications including basic scientific research, spallation neutron sources, nuclear waste transmutation, and heavy ion fusion [5]–[7]. Background electrons and plasmas are often present at the high ion current densities of practical interest. It has been recognized [8]–[17] for many years that the relative streaming motion of a charged particle beam through a background charge species provides a free energy to drive the classical two-stream instability. In addition, the presenting background plasma may act like a resistive medium, which may drive the resistive hose instability [18]–[22] in the propagating ion beam. The transverse two-stream instability [16] of ion beams propagating through a background electron cloud occurs when the charged particles (including electrons and ions) are in the collisionless regime. On the other hand, the resistive plasma medium consisted of collisional electrons develops the resistive hose instability in the ion beam [20] The transverse two-stream and resistive hose instabilities in the propagating ion beams appear fundamentally different from each other, although they are in common oscillating transversely. It is, therefore, needed to find the information how one instability mechanism evolves to the other. In this context, we develop an instability theory of a propagating ion beam through a plasma medium, assuming that the transverse conductivity of the plasma can change from zero to infinity. A general dispersion relation of the transverse instability in the ion beam will be derived in terms of the transverse conductivity of the background plasma. The general dispersion relation recovers that of the electron-ion two-stream instability in the limit of zero transverse conductivity. It is also shown that the dispersion relation of the resistive-hose instability will be obtained when the transverse conductivity goes infinity.

Basic assumptions and equilibrium properties of an intense ion beam propagating through a background plasma are presented in Section II, assuming that the beam ions are in monochromatic. The background plasma provides a conductivity tensor, which has transverse and longitudinal elements. Stability analysis is carried out in Section III in terms of the transverse conductivity $\sigma_\perp$. Coupled eigenvalue equations (32) and (33) are obtained for the flat-top density profiles of beam ions and plasma electrons. The dispersion relation [see (39)] of the transverse instability in an intense ion beam propagating through a background plasma is derived in Section III, which is one of the main results in this paper and can be used to investigate stability properties of the electron-ion two-stream instability in an intense ion beam over a broad range of system parameters, including the plasma conductivity $(4\pi\sigma_\perp/\omega)$, the magnetic decay time τ_d and fractional charge neutralization f. Finally, it is shown in Section IV that the obtained dispersion relation recovers the previous one [16], [17] of the electron-ion two-stream instability in the limit of $\sigma_\perp \rightarrow 0$. On the other hand, the dispersion relation [19] of the resistive-hose instability is recovered when $\sigma_\perp \rightarrow \infty$. Influence of the finite transverse conductivity $\sigma_\perp$ on the resistive hose stability properties are briefly investigated in Section IV for a finite pulse size of the ion beam propagating through a plasma channel. As expected, growth rate of the resistive hose instability in an ion beam decreases considerably as the transverse conductivity $4\pi\sigma_\perp/\omega$ decreases from infinity.

II. Basic Assumptions and Equilibrium Properties

The equilibrium configuration consists of an intense ion beam with radius r_b that propagates in the z direction with directed kinetic energy $(\gamma_b - 1)m_b c^2$ through a perfectly conducting cylinder with wall radius r_w. The ion beam propagates through background (stationary) electrons with characteristic directed axial momentum $\gamma_b m_b \beta_b c$ in the z direction, where $V_{\rm b} = \beta_b c =$

Manuscript received August 28, 2003; revised November 12, 2003. This work was supported in part by the Department of Energy. The work of H. S. Uhm was supported in part by Plasma and Fusion User Development Program.

H. S. Uhm is with the Department of Molecular Science and Technology, Ajou University, Suwon 442-749, Korea (e-mail: hsuhm@ajou.ac.kr.

R. C. Davidson is with the Plasma Physics Laboratory, Princeton University, Princeton, NJ 08543 USA.

Digital Object Identifier 10.1109/TPS.2004.827575

const. is the average axial velocity, and $\gamma_b = (1-\beta_b^2)^{-2}$ is the relativistic mass factor. In order to simplify the analysis, it is assumed that the background column of electrons also has the radius r_b. In the context of the smooth-focusing approximation, the beam ions are radially confined by the applied transverse focusing force modeled by [23]

$$\mathbf{F}^b_{foc} = -\gamma_b m_b \omega^2_{\beta b} \mathbf{x}_\perp \tag{1}$$

where $\mathbf{x}_\perp = x\mathbf{e}_\mathrm{x} + y\mathbf{e}_\mathrm{y}$ is the transverse displacement from the beam axis, m_b is the ion rest mass, c is the speed of light in *vacuo*, and $\omega_{\beta b} = const.$ is the effective betatron frequency for transverse ion motion in the applied focusing field. The equilibrium and stability analyses are carried out by using cylindrical polar coordinates (r, θ, z), where the z axis is along the beam propagation direction, and r is the radial distance from the z axis. Both the ion beam and background electrons (in equilibrium), are assumed to be azimuthally symmetric $(\partial/\partial\theta = 0)$ and axially uniform $(\partial/\partial z = 0)$. As for the background electrons, to the extent that the beam ion density exceeds the background electron density, the space-charge force on an electron, $\mathbf{F}^\mathrm{e}_\mathrm{s} = \mathrm{e}\boldsymbol{\nabla}\phi$, provides transverse confinement of the background electrons by the electrostatic space-charge potential $\phi(\boldsymbol{x}, t)$. However, for completeness, the present analysis also incorporates the effects of an *applied* transverse focusing force on the electrons modeled by $\mathbf{F}^\mathrm{e}_\mathrm{foc} = -m_\mathrm{e}\omega^2_{\beta\mathrm{e}}\mathbf{x}_\perp$, where m_e is the electron rest mass, and $\omega_{\beta e} = const.$ is the effective betatron frequency for transverse electron motion in the applied focusing field. It is further assumed that the ion motion in the beam frame is nonrelativistic, and that the transverse momentum components of a beam ion, p_x and p_y, and the characteristic spread in axial momentum, $\delta p_z = p_z - \gamma_b m_b \beta_b c$, are small in comparison with the directed axial momentum $\gamma_b m_b \beta_b c$.

In order to investigate effects of the plasma conductivity on the electron-ion two-stream instability, we assume that a plasma column with radius r_b coexists with the ion beam. The plasma column consists of the background electrons and also of neutrals. The plasma conductivity $\boldsymbol{\sigma}$ in general is a very complicated tensor of the plasma density, wave oscillation-frequency and neutral species including the collisional frequency. The electron motions in the background plasma are subjected to the external focusing force and also to the force generated by the self-fields from the ion-beam and electron column. In this regard, electrons cannot move freely, thereby developing tensor conductivity in general. A detail investigation of the conductivity is beyond the scope of present study. In order to make the subsequent calculation analytically tractable, we assume that the conductivity tensor is expressed as

$$\boldsymbol{\sigma}(r) = \begin{pmatrix} \sigma_\perp & 0 & 0 \\ 0 & \sigma_\perp & 0 \\ 0 & 0 & \sigma_\parallel \end{pmatrix} \tag{2}$$

for the radial coordinate r less than the beam radius r_b, and $\boldsymbol{\sigma} = 0$, otherwise. The tensor element $\sigma_\perp$ and $\sigma_\parallel$ are assumed to be constant values, although they can be a complicated function of system parameters.

Under the equilibrium assumption that the distribution function for the beam ions and background electrons are axisymmetric and spatially uniform in the axial direction, we recognize that the total transverse energies and axial momentum of the beam ions and background electrons are approximate constants of the motion in the equilibrium fields [16] For present purposes, the equilibrium distribution functions for the beam ions and the background electrons are taken to be [16]

$$\begin{aligned} F^0_b(H_{\perp b}, p_z) &= \frac{n_b}{2\pi\gamma_b m_b}\delta(H_{\perp b} - T_{\perp b})G_b(p_z) \\ F^0_e(H_{\perp e}, p_z) &= \frac{n_e}{2\pi m_e}\delta(H_{\perp e} - T_{\perp e})G_e(p_z). \end{aligned} \tag{3}$$

Here, n_b and n_e are the on axis ion and electron number densities, respectively, $T_{\perp\mathrm{b}}$ and $T_{\perp\mathrm{e}}$ are positive constants, and $H_{\perp\mathrm{b}}$ and $H_{\perp\mathrm{e}}$ are the single-particle Hamiltonians defined by

$$\begin{aligned} H_{\perp b} &= \frac{1}{2\gamma_b m_b}p^2_\perp + \frac{1}{2}\gamma_b m_b \omega^2_{\beta b} r^2 + Z_b e[\Psi_0(r) - \Psi_{0m}] \\ H_{\perp e} &= \frac{1}{2m_e}p^2_\perp + \frac{1}{2}m_e\omega^2_{\beta e}r^2 - e[\phi_0(r) - \phi_{0m}] \end{aligned} \tag{4}$$

where $Z_b e$ is the ion charge, $-e$ is the electron charge, $\Psi_0(r)$ is defined by $\Psi_0(r) = \phi_0(r) - \beta_b A_\mathrm{z}(r)$, $\phi_0(r)$ is the equilibrium electrostatic potential, and $A_\mathrm{z}(r)$ is the axial component of the equilibrium magnetic potential. In (4), $r = (x^2 + y^2)^{1/2}$ is the radial distance from the beam axis, and the axial momentum distributions are normalized according to

$$\int_{-\infty}^{\infty} G_b(p_z) d\, p_z = 1 = \int_{-\infty}^{\infty} G_e(p_z) d\, p_z. \tag{5}$$

The equilibrium self-field potentials $\Psi_0(r)$ and $\boldsymbol{\phi}_0(r)$ occurring in (4) are calculated self-consistently from [16]

$$\begin{aligned} \frac{1}{r}\frac{\partial}{\partial r}r\frac{\partial}{\partial r}\Psi_0(r) &= -4\pi e\left[\frac{Z_b}{\gamma_b^2}n^0_b(r) - n^0_e(r)\right] \\ \frac{1}{r}\frac{\partial}{\partial r}r\frac{\partial}{\partial r}\phi_0(r) &= -4\pi e\left[Z_b n^0_b(r) - n^0_e(r)\right] \end{aligned} \tag{6}$$

and the equilibrium ion and electron density profiles, $n^0_\mathrm{b}(r)$ and $n^0_\mathrm{e}(r)$, are defined by

$$\begin{aligned} n^0_b(r) &= \int d^3p\, F^0_b(H_{\perp b}, p_z), \\ n^0_e(r) &= \int d^3p\, F^0_e(H_{\perp e}, p_z). \end{aligned} \tag{7}$$

The constants $\Psi_{0\mathrm{m}}$ and $\boldsymbol{\phi}_{0m}$ in (4) are the on axis $(r = 0)$ values of the self-field potentials, $\Psi_0(r)$ and $\boldsymbol{\phi}_0(r)$, and Z_b is the ionization state of the ions, which is included here to extend the analysis to beam ions with a higher charge state than $Z_\mathrm{b} = 1$. Finally, in (4) and (6), it has been assumed that the equilibrium axial current, $J^0_z(r) = Z_b e n^0_\mathrm{b} V^0_\mathrm{zb}$, is carried by the beam ions, with $V^0_\mathrm{ze} = \beta_\mathrm{e} c = 0$.

In order to simplify subsequent analysis, we assume that the ion beam and background electrons have overlapping density

profiles. Substituting (3) into (7), and making use of (4), (5) and (6), we obtain the step-function density profiles

$$n_b^0(r) = \frac{n_e^0(r)}{Z_b f} = \begin{cases} n_b = \text{const.}, & 0 \le r < r_b, \\ 0, & r_b < r \le r_w \end{cases} \tag{8}$$

where $f = n_e/Z_b n_\mathrm{b} = const.$ is the fractional charge neutralization by the background electrons. In (8), the equilibrium beam radius r_b is defined by

$$r_b^2 = 2\frac{T_{\perp b}}{\gamma_b m_b \nu_b^2} = 2\frac{T_{\perp e}}{m_e \nu_e^2} \tag{9}$$

where the (depressed) betatron frequencies, v_b and v_e in (8) for the beam ions and background electrons are defined by [16]

$$\begin{aligned} \nu_b^2 &= \omega_{\beta b}^2 - \frac{\omega_{pb}^2}{2}\left(\frac{1}{\gamma_b^2} - f\right), \\ \nu_e^2 &= \omega_{\beta e}^2 + \frac{\omega_{pb}^2}{2}\frac{\gamma_b m_b}{Z_b m_e}(1-f). \end{aligned} \tag{10}$$

The constant $f = n_e/Z_b n_b$ in (8) and (10) represents the fractional charge neutralization provided by the background electrons. The quantity ω_{pb}^2 occurring in (10) is the on-axis relativistic beam plasma frequency-squared defined by $\omega_{pb}^2 = 4\pi n_\mathrm{b} Z_\mathrm{b}^2 e^2/\gamma_b m_b$. As expected, the (depressed) betatron frequencies in (10) for the ions and electrons inside the beam are constants (independent of radial coordinate r) for the step-function density profiles in (8).

III. Dispersion Relation of Electron-Ion Instability for Arbitrary Value of Plasma Conductivity

The dispersion relation of the electron-ion two-stream instability is obtained in this section for an arbitrary value of the plasma conductivity. We now make use of linearized Vlasov-Maxwell equations [1] to develop a theoretical model of the two-stream instability for perturbations about the equilibrium described by (3). In the subsequent analysis, we adopt a normal mode approach in which all perturbed quantities are assumed to vary with θ, z, and t according to

$$\delta\xi(r,\theta,z,t) = \xi_1(r)\exp\left[i(\theta + kz - \omega t)\right] \tag{11}$$

for garden hose (kink-mode) perturbations. Here, ω and k are the complex eigenfrequency and axial wavenumber of the perturbation, with $Im\omega > 0$ corresponding to temporal growth. We also consider axial wavelengths that are long and frequencies that are low compared with quantities that characterize the beam radius, i.e.,

$$|kr_b| \ll 1, \quad |\omega r_b| \ll c. \tag{12}$$

Furthermore, the present stability analysis assumes electrostatic perturbations with sufficiently high frequency that $|\omega/k - \beta_b c| \gg v_{Tbz}$ and $|\omega/k| \gg v_{Tez}$, where $v_{Tbz} = (2T_{bz}/\gamma_\mathrm{b}^3 m_\mathrm{b})^{1/2}$ and $v_{Tez} = (2T_{ez}/m_\mathrm{e})^{1/2}$ are the characteristic axial thermal speeds of the beam ions and the background electrons, respectively. Indeed, for present purposes, we assume $G_b(p_z) = \delta(p_z - \gamma_\mathrm{b} m_b \beta_b c)$ and $G_e(p_z) = \delta(p_z)$, which correspond to beam ions and background electrons that are 'cold' in the axial direction.

The perturbed electric and magnetic fields, $\mathbf{E_1}(\mathbf{x})$, and $\mathbf{B_1}(\mathbf{x})$, can be expressed in terms of perturbed magnetic and electric potentials $\mathbf{A}_{z1}(\mathbf{x})$ and $\phi_1(\mathbf{x})$

$$\begin{aligned} \mathbf{B}_1(\mathbf{x}) &= \nabla \times \mathbf{A}_1(\mathbf{x}) \\ \mathbf{E}_1(x) &= i\left(\frac{\omega}{c}\right)\mathbf{A}_1(\mathbf{x}) - \nabla\phi_1(\mathbf{x}). \end{aligned} \tag{13}$$

Introducing the Lorentz gauge

$$\nabla\cdot\mathbf{A}_1(\mathbf{x}) - i\left(\frac{\omega}{c}\right)\phi_1(\mathbf{x}) = 0 \tag{14}$$

into the Maxwell equations, and using (12), the perturbed potentials in (13) satisfy

$$\begin{aligned} \nabla_\perp^2\mathbf{A}_1(\mathbf{x}) &= -\left(\frac{4\pi}{c}\right)\mathbf{J}_1(\mathbf{x}) \\ \nabla_\perp^2\phi_1(\mathbf{x}) &= -4\pi\rho_1(\mathbf{x}) \end{aligned} \tag{15}$$

where $\rho_1(\mathbf{x})$ and $\mathbf{J}_1(\mathbf{x})$ are the perturbed charge and current densities, which must be determined self-consistently, and the subscript $\perp$ denotes transverse components. The perturbed current density $\mathbf{J}_\mathrm{p}(\mathbf{x})$ contributed by the background plasma is given by

$$\mathbf{J}_p(\mathbf{x}) = \sigma(r)\mathbf{E}_1(\mathbf{x}) = \sigma\left[i\left(\frac{\omega}{c}\right)\mathbf{A}_1(\mathbf{x}) - \nabla\phi_1(\mathbf{x})\right] \tag{16}$$

where $\boldsymbol{\sigma}(r)$ is the conductivity tensor of the background plasma defined in (2).

The axial component $J_{pz}(r)$ of the perturbed current density contributed by the background plasma is expressed as

$$J_{pz}(r) = i\left(\frac{\omega}{c}\right)\sigma_{||}\left[A_{z1}(r) - \left(\frac{kc}{\omega}\right)\phi_1(r)\right] \tag{17}$$

from (2) and (16) for the radial coordinate r satisfying $r < r_b$ and $J_{pz}(r) = 0$ otherwise. The axial component $A_{1z}(r)$ of the perturbed magnetic potential satisfies

$$\begin{aligned} &\frac{d}{dr}\frac{1}{r}\frac{d}{dr}rA_{z1}(r) + \frac{4\pi i\omega\sigma_{||}}{c^2}\left[A_{z1}(r) - \frac{kc}{\omega}\phi_1(r)\right] \\ &\quad = -\left(\frac{4\pi}{c}\right)J_{bz}(r) \\ &\quad = -4\pi Z_b e\beta_b n_{b1}(r) \end{aligned} \tag{18}$$

for $r \le r_b$ and

$$\frac{d}{dr}\frac{1}{r}\frac{d}{dr}rA_{z1}(r) = 0 \tag{19}$$

for $r_b < r \le r_w$. Equations (18) and (19) are obtained from (15) and (17). The perturbed current density $J_{bz}(r)$ in (18) is contributed by the ion beam. The background electrons may not directly contribute into the perturbed current density, although they may participate in generation of the perturbed current density J_{pz} of the background plasma. The perturbed ion-beam density $n_{b1}(r)$ in (18) will be determined self-consistently.

The perturbed charge density $\rho_p(\boldsymbol{x})$ contributed by the background plasma is related to the perturbed current density $\mathbf{J}_p(\mathbf{x})$ by the continuity equation $-i\omega\rho_p + \boldsymbol{\nabla}\cdot\mathbf{J}_p = 0$. For the low-frequency long-wavelength perturbations satisfying

(12), the perturbed charge density $\rho_p(\mathbf{x})$ contributed by the background plasma can be expressed as

$$\rho_p(\mathbf{x}) = \frac{1}{c}\nabla_\perp \cdot \sigma_\perp \mathbf{A}_\perp + \frac{i}{\omega}\nabla_\perp \cdot \sigma_\perp \nabla_\perp \phi \tag{20}$$

from (16) and continuity equation. Making use of Lorentz gauge in (14), we can show that the term proportional to $\mathbf{A}_\perp$ in the right-hand side (RHS) of (20) is negligibly small in comparison with the term proportional to ϕ because of the low-frequency perturbations. The corrections associated with this term is order of $(\omega r_b/c)^2$. Therefore, the perturbed electric potential $\phi_1(r)$ in (15) satisfies

$$\frac{1}{r}\frac{d}{dr}\left[r\left(1+\frac{4\pi i\sigma_\perp}{\omega}\right)\frac{d}{dr}\phi_1(r)\right] - \frac{1}{r^2}\left(1+\frac{4\pi i\sigma_\perp}{\omega}\right)\phi_1(r) = -4\pi e\left[Z_b n_{b1}(r) - n_{e1}(r)\right] \tag{21}$$

for $r \le r_b$ and

$$\frac{1}{r}\frac{d}{dr}\left[r\frac{d}{dr}\phi_1(r)\right] - \frac{1}{r^2}\phi_1(r) = 0 \tag{22}$$

for $r_b < r \le r_w$.

The perturbed densities $n_{b1}(r)$ and $n_{e1}(r)$ in (21) of the beam ions and background electrons can be obtained from the linearized Vlasov equations for δF_b and δF_e. For example, the perturbed ion beam density $n_{\mathrm{b1}}(r)$ is calculated from

$$n_{b1}(r) = \int d^3p \delta F_b. \tag{23}$$

In (23), δF_b is the perturbed ion beam distribution function calculated by the method of the characteristics [1] which can be expressed as [16]

$$\delta F_b(\mathbf{x},\mathbf{p},t) = Z_b e G_b(p_z)\frac{\partial}{\partial H_{\perp b}}F_{b0}(H_{\perp b}) \times \int_{-\infty}^{t} dt' \frac{\mathbf{p}'_\perp}{\gamma_b m_b}\cdot\nabla_\perp \delta\psi(\mathbf{x}',t') \tag{24}$$

where use has been made of (12). Here, $\mathbf{x}'(t')$ and $\mathbf{p}'(t')$ are the particle trajectories in the equilibrium field configuration that pass through the phase space point $(\mathbf{x}, \mathbf{p})$ at time $t' = t$.

We note from (24) that the time integral requires information on the particle orbits in the equilibrium fields. A determination of the particle orbit in the equilibrium fields, generated by the self-field potentials $\Psi_0(\mathbf{x})$ and $\phi_0(\mathbf{x})$ in (6), is difficult for general equilibrium profiles. Moreover, (24) contains an integral over the unperturbed orbits of the (yet unknown) eigenfunction $\delta\psi$, which makes (18) and (21) generally intractable analytically. This difficulty is fundamental, reflecting the fact that individual particle orbits span the beam cross-section, communicating information about the perturbation from one value of r to another. However, the particle motion in the equilibrium field configuration generated by the step-function density profile in (8) can be determined exactly and are given by [16]

$$\begin{aligned} x'(\tau) &= \frac{p_\perp}{\gamma_j m_j \nu_j}\cos\varphi \sin\nu_j\tau + r\cos\theta\cos\nu_j\tau \\ y'(\tau) &= \frac{p_\perp}{\gamma_j m_j \nu_j}\sin\varphi \sin\nu_j\tau + r\sin\theta\cos\nu_j\tau \end{aligned} \tag{25}$$

where ν_j is the (depressed) betatron frequency defined in (10), and $\tau = t' - t$ is the displaced time variable. The boundary condition of the particle orbit are $x'(\tau = 0) = x = r\cos\theta$ and $y'(\tau = 0) = y = r\sin\theta$. The transverse momentum $p_\perp$ is defined by $p_\perp = (p_x^2 + p_y^2)^{1/2}$. The beam ions and the background electrons execute the simple harmonic orbits described by (25) over the beam cross-section.

In addition, the eigenfunctions (the perturbed potentials) of the garden-hose perturbations in the step-function density profile are linearly proportional to r, forming the exact solution in the beam interior $(0 \le r < r_b)$ and generating dominant surface perturbations [16]. In this regard, the perturbed electric potential $\phi_1(r)$ and the axial component $A_{z1}(r)$ of the perturbed magnetic potential are expressed as

$$\phi_1(r) = C_e \begin{cases} r, & 0 \le r < r_b \\ \dfrac{r - \frac{r_w^2}{r}}{1 - \frac{r_w^2}{r_b^2}}, & r_b < r \le r_w \end{cases} \tag{26}$$

and

$$A_{z1}(r) = C_m \begin{cases} r, & 0 \le r < r_b \\ \dfrac{r - \frac{r_w^2}{r}}{1 - \frac{r_w^2}{r_b^2}}, & r_b < r \le r_w \end{cases} \tag{27}$$

respectively.

We now substitute the particle orbits in (25) and the eigenfunctions in (26) and (27) into (24) and obtain the perturbed distribution function δF_b by calculating along the particle trajectories. The perturbed ion-beam density $n_{b1}(r)$ is eventually calculated from (23). After carrying out a tedious but straightforward calculation, we obtain [16]

$$4\pi Z_b e n_{b1}(r) = \chi_b\left[\phi_1(r_b) - \beta_b A_{z1}(r_b)\right]\frac{1}{r_b}\delta(r - r_b) \tag{28}$$

where the ion susceptibility χ_{b} is defined by

$$\chi_b(\omega - k\beta_b c) = \frac{\omega_{pb}^2}{(\omega - k\beta_b c)^2 - \nu_b^2}. \tag{29}$$

The plasma frequency-squared ω_{pb}^2 of the beam ions is defined in (10). Similarly, the perturbed electron density n_{e1} is calculated and given by [16]

$$4\pi e n_{e1}(r) = -\chi_e(\omega)\phi_1(r_b)\frac{1}{r_b}\delta(r - r_b) \tag{30}$$

where the electron susceptibility χ_{e} is defined by

$$\chi_e(\omega) = \frac{\eta f \omega_{pb}^2}{\omega^2 - \nu_e^2} \tag{31}$$

where η is defined by $\eta = \gamma_{\mathrm{b}} m_b / Z_b m_e$ and $f = n_e/Z_b n_b$ is the fractional charge neutralization. Note that the perturbed ion and electron densities in (28) and (30) vanish except at $r = r_b$, exhibiting surface perturbations.

Substituting (28) into (18), the axial component of the perturbed magnetic potential inside ion beam is determined from

$$\frac{d}{dr}\frac{1}{r}\frac{d}{dr}rA_{z1}(r) + \frac{4\pi i\omega\sigma_\parallel}{c^2}\left[A_{z1}(r) - \frac{kc}{\omega}\phi_1(r)\right] = -\chi_b\left[\phi_1(r_b) - \beta_b A_{z1}(r_b)\right]\frac{\delta(r - r_b)}{r_b} \tag{32}$$

for $r \leq r_b$. We can also substitute (28) and (30) into (21) and find that the perturbed electric potential $\phi_1(r)$ inside the ion beam can be obtained from

$$\frac{1}{r}\frac{d}{dr}\left[r\left(1+\frac{4\pi i\sigma_\perp}{\omega}\right)\frac{d}{dr}\phi_1(r)\right]-\frac{1}{r^2}\left(1+\frac{4\pi i\sigma_\perp}{\omega}\right)\phi_1(r) = -\left[\chi_b\phi_1(r_b)-\beta_b\chi_b A_{z1}(r_b)+\chi_e\phi_1(r_b)\right]\frac{\delta(r-r_b)}{r_b} \quad (33)$$

for $r \leq r_b$. Equations (32) and (33) are the coupled eigenvalue equations inside the beam.

The perturbed electric potential ϕ_1 in (26) is continuous at $r = r_b$. However, its radial derivative is discontinuous at $r = r_b$. The remaining boundary condition relating $\phi_{\rm i}$ and $\phi_{\rm o}$ is obtained by multiplying the eigenvalue equation (33) by r, integrating across the surface of the ion beam from $r = r_b(1-\varepsilon)$ to $r = r_b(1+\varepsilon)$, and taking the limit $\varepsilon \to 0_+$. Here $\phi_{\rm i}$ is the potential inside beam and $\phi_{\rm o}$ is the potential outside the beam. We then obtain

$$r_b\left[\frac{\partial}{\partial r}\phi_o(r)\right]_{r_b}-r_b\left(1+\frac{4\pi i\sigma_\perp}{\omega}\right)\left[\frac{\partial}{\partial r}\phi_i(r)\right]_{r_b} = -\left[\chi_b\phi(r_b)-\beta_b\chi_b A_{z1}(r_b)+\chi_e\phi_1(r_b)\right]. \quad (34)$$

Equation (34) relates the discontinuity in the perturbed radial electric field at $r = r_b$ to the perturbed charge density at the surface of the ion beam. Substituting (26) into (34), the condition for a nontrivial solution ($C_e \neq 0$) can be expressed as

$$\left(\frac{4\pi i\sigma_\perp}{\omega}+2g_f\right)\phi_1(r_b)=\chi_b\left[\phi_1(r_b)-\beta_b A_{z1}(r_b)\right]+\chi_e\phi_1(r_b) \quad (35)$$

where the geometrical factor g_f defined by

$$g_f\left(\frac{r_b}{r_w}\right)=\frac{1}{1-\frac{r_b^2}{r_w^2}} \quad (36)$$

is order unity unless the wall radius approaches very close to the beam radius. We remind the reader that the RHS of (35) represents the perturbed surface charge that generates the radial electric field inside the beam. The electric potential ϕ_1 in the left-hand side of (35) is the potential strength caused by this surface charge. Note that the geometrical factor g_f increases to infinity, as the conducting wall approaches the beam radius. The surface charge is, therefore, neutralized by an approaching conducting wall, eliminating the perturbed electric potential. We also note from (35) that the surface charge is also neutralized by the high conductivity plasma of $|4\pi i\sigma_\perp/\omega| \gg 1$. The conducting current again neutralizes the surface charge, deceasing the electric field inside the beam.

The perturbed magnetic potential in (27) is not an exact solution of the eigenvalue equation (32) because of the magnetic decay term proportional to σ_{11}. However, (27) is a good solution by the variational approximation [19]. In order to find an approximate dispersion relation which includes the influence of the magnetic decay, we multiply (32) by $rA_{z1}(r)$ and integrate over r from $r = 0$ to $r = r_w$. It was shown in a previous study [19] that if a trial function A_t is substituted in the integrals, this procedure gives a dispersion relation that is accurate to second order in the error in A_t. Thus, the procedure can be described as a variational approximation, although it does not give a lower bound, because the differential operator is non-Hermitian. The result is

$$2g_f A_{z1}(r_b)-2i\omega\tau_d\left[A_{z1}(r_b)-\left(\frac{kc}{\omega}\right)\phi_1(r_b)\right] = \beta_b\chi_b\left[\phi_1(r_b)-\beta_b A_{z1}(r_b)\right] \quad (37)$$

where the magnetic decay time $\tau_{\rm d}$ is defined by

$$\tau_d=\frac{1}{2}\frac{\pi\sigma_{\|}r_b^2}{c^2} \quad (38)$$

which is essentially a decay time for the perturbed current.

We obtain the dispersion relation by eliminating $\phi_1(r_b)$ and $A_{z1}(r_b)$ from (35) and (37). The resultant dispersion relation is

$$\left(2g_f+\frac{4\pi i\sigma_\perp}{\omega}-\chi_b-\chi_e\right)\left(2g_f+\beta_b^2\chi_b-2i\omega\tau_d\right) = -\beta_b\chi_b(\beta_b\chi_b-2i\tau_d kc) \quad (39)$$

which is one of the main results in this paper and can be used to investigate stability properties of the electron-ion two-stream instability in an intense ion beam over a broad range of system parameters, including the plasma conductivity ($4\pi\sigma_\perp/\omega$), the magnetic decay time $\tau_{\rm d}$ and fractional charge neutralization f.

IV. The Resistive-Hose and Electon-Ion Two-Stream Instabilities

If the ion beam propagates through a tenuous background electron cloud, the electron density is considerably less than the ion density and, therefore, the transverse and longitudinal conductivities may be negligibly small ($4\pi\sigma_\perp/\omega \to 0$ and $\tau_d \to 0$). In this limit, the dispersion relation in (39) is simplified to

$$\left(2g_f-\frac{\chi_b}{\gamma_b^2}\right)(2g_f-\chi_e)=\chi_b\chi_e \quad (40)$$

which is equivalently expressed as

$$\left[2g_f-\frac{\frac{\omega_{pb}^2}{\gamma_b^2}}{(\omega-k\beta_b c)^2-\nu_b^2}\right]\left[2g_f-\frac{\eta f\omega_{pb}^2}{\omega^2-\nu_e^2}\right] = \frac{\eta f\omega_{pb}^4}{\left[(\omega-k\beta_b c)^2-\nu_b^2\right](\omega^2-\nu_e^2)}. \quad (41)$$

In obtaining (41), use has been made of the ion and electron susceptibilities in (29) and (31). Stability properties of the electron-ion two-stream instability described by the dispersion relation in (41) has been extensively investigated in the previous studies [16]. Particularly, influence of the fractional charge neutralization caused by the electron cloud along the ion beam propagation has been well documented. We, therefore, strongly urge the reader to review [16].

It is instructive to investigate hose instability in limiting cases by making use of the dispersion relation in (39). Let us assume that the ion beam propagates through relatively high-density neutrals. The beginning portion of the ion beam may ionize neutrals creating a high-density plasma and the later portion of the beam may propagate through this high-density plasma channel. Although the plasma electrons may be highly collisional with neutrals, their density can be considerably higher than the ion density. The electron plasma frequency is much higher than the

ion plasma frequency. The typical oscillation frequency ω is on the order of the ion plasma frequency. Therefore, the ion beam may propagate a high-conductivity plasma channel characterized by $4\pi\sigma_\perp \gg |\omega|$. Due to the high density of electrons, the fractional charge neutralization f in (10) is unity and therefore, the depressed betatron frequency ν_b of beam ions is obtained from $\nu_b^2 = \omega_{\beta b}^2 + \beta_b^2\omega_{pb}^2/2$. In this limit, the dispersion relation in (39) is simplified to

$$i\omega\tau_d = g_f + \frac{\frac{\omega_{pb}^2\beta_b^2}{2}}{\Omega^2 - \nu_b^2} \tag{42}$$

which is a typical dispersion relation of the resistive hose instability obtained in the previous studies [19]. Here, $\Omega = \omega - k\beta_b c)$ is the Doppler-shifted frequency. In obtaining (42), use has been made of the ion susceptibility in (29). We recommend the readers to review the previous literatures [19] for detailed stability properties of the resistive hose instability. As mentioned earlier, the high transverse conductivity neutralizes the surface charge, eliminating the electric potential $\phi_1(r)$ in the eigenvalue equation (32), which can then be solved by only one eigenfunction $A_{z1}(r)$. Therefore, the resistive hose instability is fully described by the axial component of the perturbed magnetic potential.

A finite size beam pulse is often required to propagate to a target in practical applications. Although the beam head may be at the target, the tail of the beam pulse may deviate from the proposed path due to perturbations that are initiated at the beam head and propagate through the beam pulse, growing during the propagation. In the coordinate τ defined by

$$\tau = t - \frac{z}{\beta_b c} \tag{43}$$

represents the distance (in unit of $\beta_b c$) from the beam head to position z. Then, the perturbed quantities in the beam are assumed to vary according to $\exp[i(\theta - \Omega z/\beta_b c - \omega\tau)]$. If each beam segment in the beam pulse is taken to oscillate at a fixed real axial wave number $\Omega/\beta_b c$, then ω in (42) represent oscillation and growth (or damping) of the perturbation as one moves backward from the head of the beam. Equation (42) determines the dependence of ω on Ω (assuming real). It is obvious from (42) that the complex frequency ω is purely imaginary for real values of Ω. Moreover, instability ($\mathrm{Im}\omega > 0$) occurs only over a bounded range of Ω^2 satisfying

$$\nu_b^2 - \frac{\omega_{pb}^2\beta_b^2}{2g_f} < \Omega^2 < \nu_b^2. \tag{44}$$

The growth rate $\mathrm{Im}\omega$ approaches (unphysically) infinity as Ω^2 approaches the betatron frequency squared from below, i.e., $\Omega^2 \to {\nu_\mathrm{b}}^2$. This occurs for the flattop density profile in (8) for the choice of distribution function in (3), because all particles in the beam are in resonance with the wave at this frequency. Keep in mind from (10) and (25) that all beam particles in a flattop density profile execute transverse oscillations at the betatron frequency $\nu_b = \mathrm{const.}$ defined in (10). Therefore, choosing $\Omega = \nu_b$ would cause a very strong growth of the perturbation that propagates from beam head to tail. For (more physical) rounded beam profiles, however, the growth rate for the resistive hose instability is finite [22] for any value of Ω because the beam particles in these profiles oscillate with different betatron frequencies determined by their position.

Influence of the plasma conductivity on the ion beam propagation can be investigated by numerically analyzing (39) in general. There are so many ways to investigate properties of the ion beam propagation through a plasma channel. We, therefore, urge the readers to investigate (39), customizing the physical parameters for their specified needs. However, we may investigate properties of the resistive hose instability of ion beam propagation in the remainder of this section as an example. Stability properties of a finite beam pulse where the head perturbation propagates toward tail as shown in (42) are investigated here. After carrying out a straightforward algebraic manipulation, we obtain

$$i\omega\tau_d = g_f + \frac{\beta_b^2\chi_b}{2} + K - iL \tag{45}$$

from (39) where the functions K and L are defined by

$$K = \frac{\frac{\beta_b^2\chi_b^2(2g_f - \chi_b - \chi_e)}{2}}{(2g_f - \chi_b - \chi_e)^2 + \left(\frac{4\pi\sigma_\perp}{\omega}\right)^2} \tag{46}$$

and

$$L = \frac{\beta_b\chi_b\left[\frac{2\pi\sigma_\perp\beta_b\chi_b}{\omega} + kc\tau_d(2g_f - \chi_b - \chi_e)\right]}{(2g_f - \chi_b - \chi_e)^2 + \left(\frac{4\pi\sigma_\perp}{\omega}\right)^2} \tag{47}$$

respectively. The growth rate $\omega_i = \mathrm{Im}\omega$ and real oscillation frequency $\omega_r = \mathrm{Re}\omega$ are defined by $\omega = \omega_r + i\omega_\mathrm{i}$, obtained from the dispersion relation in (45), and given by

$$\omega_i = lm\omega = -\frac{g_f - K - \beta_b^2\chi_b}{2} \tag{48}$$

and

$$\omega_r = \mathrm{Re}\omega = -L \tag{49}$$

respectively. Note from (46) and (47) that the functions K and L approach zero, recovering (42), as the transverse conductivity $\sigma_\perp$ increases to infinity, i.e., $\sigma_\perp \to \infty$, as expected.

Equation (45) is a highly nonlinear equation of the complex frequency ω for given real values of Ω. Thus, we introduce the normalized physical parameter $4\pi\sigma_\perp/\omega$ as a real transverse conductivity parameter for convenience of the subsequent analysis, where (45) becomes a simple equation of the parameter $4\pi\sigma_\perp/\omega$. The ion betatron frequency ν_b depends strongly to the ion focusing force $(\omega_{\beta b})$ provided outside as shown in (10). We, therefore, assume $\omega_{pb}^2/\nu_b^2 = 1$ as an example for presentation purpose. The ion kinetic energy determines the ion beam velocity, which can be large or small depending on experimental conditions. We assume $\omega_{pb}^2\beta_b^2/2\nu_b^2 = 0.05$, saying that $\beta_b^2 = 0.1$. Assuming that the conducting tube wall is far away from the propagating ion beam, the geometrical factor g_f can be given by $g_f = 1$. The electron betatron frequency (ν_e) can be any number depending on the system configuration. The electron susceptibility χ_e in (31) is a function of the electron focusing force $(\omega_{\beta e})$, the ion electron mass ratio (m_i/m_e), and the electron density, etc. Thus, The electron susceptibility χ_e can be very large or very small depending on the experimental conditions, although the electron betatron frequency is much larger

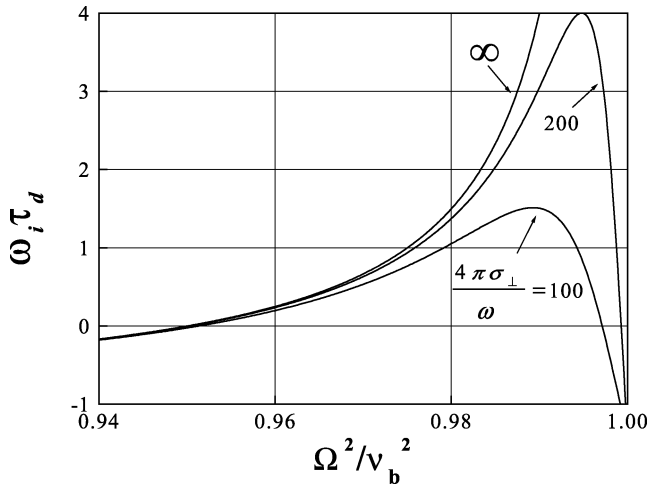

Fig. 1. Plots of the normalized growth rate $\omega_i\tau_d$ versus the normalized axial wavenumber squared Ω^2/ν_b^2 obtained numerically from (46)–(49) for several different values of the transverse conductivity parameter $4\pi\sigma_\perp/\omega$.

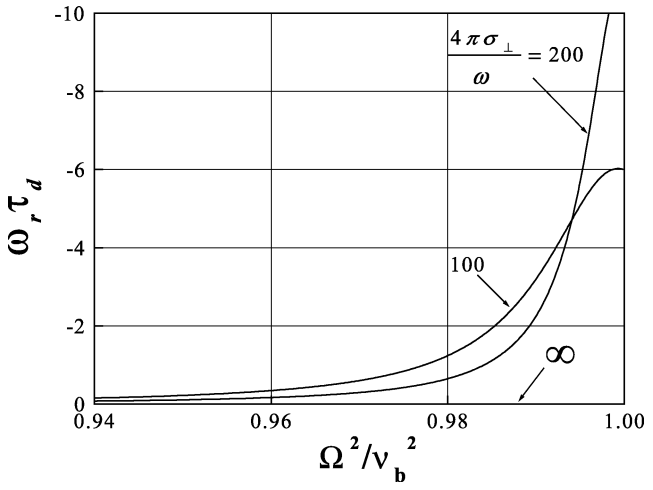

Fig. 2. Plots of the normalized real oscillation frequency $\omega_r\tau_d$ versus the normalized axial wavenumber squared Ω^2/ν_b^2 obtained numerically from (46)–(49) for several different values of the transverse conductivity parameter $4\pi\sigma_\perp/\omega$.

than the frequency ω. For purpose of the present presentation, we simply assume $\chi_e = 10$. Note from (38) that the magnetic decay time (τ_d) can be any value, which can be large or small depending on the plasma conductivity. However, it is assumed that the magnetic decay time is given to be $\nu_b\tau_d = 1$ for presentation purpose. The resistive hose instability of the ion beam propagation occurs at the high transverse conductivity in usual. We, therefore, concentrate on high values of $4\pi\sigma_\perp/\omega$ which are much larger than unity for practical applications.

Introducing all these physical parameters into (46)–(49) and carrying out numerical calculations, we obtain the normalized growth rate $\omega_i\tau_d$ and the real oscillation frequency $\omega_r\tau_d$ which are normalized by the magnetic decay time defined in (38). Shown in Fig. 1 are plots of the normalized growth rate $\omega_i\tau_d$ versus the normalized axial wavenumber squared Ω^2/ν_b^2 obtained numerically from (46)–(49) for several different values of the transverse conductivity parameter $4\pi\sigma_\perp/\omega$. Note that the growth rate for $4\pi\sigma_\perp/\omega = \infty$ in Fig. 1 is also identical to the result from (42), thereby increasing to infinity as the parameter Ω^2/ν_b^2 approaches unity as mentioned earlier. Remember that the perturbation grows only when $\omega_i\tau_d > 0$. The growth rate and the region where instability occurs in the parameter space of Ω^2/ν_b^2 deceases considerably as the transverse conductivity decreases from infinity. When the beam pulse segment moves sideway, the self magnetic field accompanying the segment stays where it was in the infinite transverse conductivity channel due to the mechanism of magnetic field frozen in an infinite conducting material. Therefore, the magnetic field pulls back the side stepped beam segment, overshooting it and imposing the perturbation growth. In this case, the beam pulse acts like a rigid body. However, some of the magnetic field lines may slip through the plasma channel following the side stepped beam segments in the case of the finite transverse conductivity. Therefore, the restoring force due to the remaining magnetic field may decreases and the perturbation growth may also reduce. This is why the growth rate deceases as the transverse conductivity decreases. Fig. 2 present plots of the normalized real oscillation frequency $\omega_r\tau_d$ versus the normalized axial wavenumber squared Ω^2/ν_b^2 obtained numerically from (46)–(49) for several different values of the transverse conductivity parameter $4\pi\sigma_\perp/\omega$. The real oscillation frequency $\omega_r\tau_d$ is zero as expected for $4\pi\sigma_\perp/\omega = \infty$. Otherwise, the real oscillation frequency is nonzero for a finite value of the transverse conductivity.

V. Conclusion

We have developed an instability theory of a propagating ion beam through a plasma medium assuming that the transverse conductivity of the background plasma can change from zero to infinity. Basic assumptions and equilibrium properties of an intense ion beam propagating through a background plasma were presented in Section II, assuming that the beam ions are in monochromatic. The background plasma provides a conductivity tensor, which has transverse and longitudinal elements. Stability analysis was carried out in Section III in terms of the transverse conductivity $\sigma_\perp$. Coupled eigenvalue equations (32) and (33) were obtained for the flat-top density profiles of beam ions and plasma electrons. The dispersion relation [see (39)] of the transverse instability in an intense ion beam propagating through a background plasma was derived in Section III, which is one of the main results in this paper and can be used to investigate stability properties of the electron-ion two-stream instability in an intense ion beam over a broad range of system parameters, including the plasma conductivity $(4\pi\sigma_\perp/\omega)$, the magnetic decay time τ_d and fractional charge neutralization f. Finally, it was shown in Section IV that the obtained dispersion relation recovers the previous one of the electron-ion two-stream instability in the limit of $\sigma_\perp \to 0$. On the other hand, the dispersion relation of the resistive-hose instability is recovered when $\sigma_\perp \to \infty$. Influence of the finite transverse conductivity on the resistive hose stability properties were briefly investigated in Section IV for a finite pulse size of the ion beam propagating through a plasma channel. As expected, growth rate of the resistive hose instability in an ion beam decreases considerably as the transverse conductivity decreases from infinity.

REFERENCES

[1] R. C. Davidson, *Physics of Nonneutral Plasmas*. Reading, MA: Addison-Wesley, 1990.

[2] A. W. Chao, *Physics of Collective Beam Instabilities in High Energy Accelerators*. New York: Wiley, 1993.

[3] M. Reiser, *Theory and Design of Charged Particle Beams*. New York: Wiley, 1994.

[4] J. D. Lawson, *The Physics of Charged-Particle Beams*. New York: Oxford Science, 1988.

[5] R. A. Jameson, *Advanced Accelerator Concepts*, J. S. Wurtele, Ed. New York: Amer. Inst. Phys., 1993, vol. 279, American Institute of Physics Conference Proceedings, p. 969.

[6] E. P. Lee and J. Hovingh, *Fusion Technol.*, vol. 15, p. 369, 1989.

[7] J. J. Barnard, T. J. Fessenden, and E. P. Lee, Eds., "Physics design and scaling of recirculating induction accelerators: from benchtop prototypes to drivers; Intense heavy ion beam transport with electric and magnetic quadrupoles; Physics design and scaling of Elise," in *Fusion Engineering and Design*, 1996, vol. 32, Proc. 1995 Int. Symp. Heavy Ion Inertial Fusion, pp. 1–620.

[8] D. G. Koshkarev and P. R. Zenkevich, "Ion resonance instability in an electron ring accelerator," *Particle Accelerators*, vol. 3, p. 1, 1972.

[9] R. C. Davidson and H. S. Uhm, "Coupled dipole oscillation of intense relativistic electron beam," *J. Appl. Phys.*, vol. 51, p. 885, 1980.

[10] ——, "Influence of finite ion larmor radius effects on the ion resonance instability in a nonneutral plasma column," *Phys. Fluids*, vol. 21, p. 60, 1978.

[11] D. Neuffer, E. Colton, D. Fitzgerald, T. Hardek, R. Hutson, R. Macek, M. Plum, H. Thiessen, and T. S. Wang, "Observations of a fast transverse instability in the PSR," *Nucl. Instrum. Methods Phys. Res.*, vol. A321, p. 1, 1992.

[12] D. Neuffer and C. Ohmori, "Calculations of the conditions for bunch leakage in the Los Alamos proton storage ring," *Nucl. Instrum. Methods Phys. Res.*, vol. A343, p. 390, 1994.

[13] M. Izawa, Y. Sato, and T. Toyomasu, "The vertical instability in a positron bunched beam," *Phys. Rev. Lett.*, vol. 74, p. 5044, 1995.

[14] J. Byrd, A. Chao, S. Heifets, M. Minty, T. O. Roubenheimer, J. Seeman, G. Stupakov, J. Thomson, and F. Zimmerman, "First observations of a 'fast beam-ion instability," *Phys. Rev. Lett.*, vol. 79, 1997.

[15] E. Keil and B. Zotter, CERN, Geneva, Switzerland, Rep. CERN_ISR-TH/71-58, 1971.

[16] R. C. Davidson, P. H. Stoltz, and T. S. Wang, "Kinetic description of electron-proton instability in high-intensity proton linacs and storage rings based on the Vlasov-Maxwell equations," *Phys. Rev. Special Topics, Accel. and Beams*, vol. 2, p. 054 401, 1999.

[17] R. C. Davidson and H. S. Uhm, "Effects of the solenoid focusing field on the electron-ion two-stream instability in high intensity ion beams," *Phys. Lett.*, vol. A 285, p. 88, 2001.

[18] E. P. Lee, "Resistive hose instability of a beam with the Bennett profile," *Phys. Fluids*, vol. 21, p. 1327, 1978.

[19] H. S. Uhm and R. C. Davidson, "Effects of the electron collisions on the resistive instability in intense charged particle beams propagating through a background plasmas," *Phys. Rev. Special Topics (Accel. Beam)*, vol. 6, 2003.

[20] H. S. Uhm and M. Lampe, "Theory of the resistive hose instability in relativistic electron beams," *Phys. Fluids*, vol. 23, p. 1574, 1980.

[21] ——, "Stability properties of azimuthally symmetric perturbations in an intense electron beam," *Phys. Fluids*, vol. 24, p. 1553, 1981.

[22] G. Joyce and M. Lampe, "Numerical simulation of the axisymmetric hollowing instability of a propagating beam," *Phys. Fluids*, vol. 26, p. 3377, 1983.

[23] H. S. Uhm and R. C. Davidson, "Low-frequency flute instabilities in intense nonneutral electron and ion beams," *Phys. Fluids*, vol. 23, p. 1586, 1980.

Han S. Uhm was born November 3, 1942 in Chonju, Korea. He received the Ph.D. degree from University of Maryland, College Park, in 1976.

From 1978 to 1999, he was with the Naval Surface Warfare Center. He is currently a Professor at Ajou University, Paldal-ku Suwon, South Korea. His research interests include: charged particle beams (charged particle-beam propagation in air, beam properties in particle accelerators, collective ion acceleration and high-power electrical pulse system); high-power microwave generations (gyrotron, magnetron, free electron laser and klystron); plasma material processing (large-volume plasma generations for plasma processing, focused ion-beam generation, and plasma ion implantation for wear and corrosion resistance materials); neutron transport physics (neutron radiography and shallow-water mine detection); plasma chemistry (plasma-assisted chemical vapor elimination and air purification).

Ronald C. Davidson He received the B.Sc. degree from McMaster University, Hamilton, ON, Canada, in 1963, and the Ph.D. degree from Princeton University, Princeton, NJ, in 1966.

has been Professor of Astrophysical Sciences at Princeton University since 1991, and was Director of the Princeton Plasma Physics Laboratory from 1991–1996. He was Assistant Research Physicist at the University of California at Berkeley from 1966–1968, an Assistant Professor of Physics at the University of Maryland, College Park, from 1968–1971, an Alfred P. Sloan Foundation Fellow from 1970–1972, an Associate Professor of Physics from 1971–1973, a Professor of Physics at the University of Maryland from 1973–1978, and Professor of Physics at the Massachusetts Institute of Technology, Cambridge, from 1978–1991. He has made numerous fundamental theoretical contributions to several areas of pure and applied plasma physics, including nonneutral plasmas, nonlinear effects and anomalous transport, kinetic equilibrium and stability properties, intense charged particle beam propagation in high-energy accelerators, and coherent radiation generation by relativistic electrons. He is the author of more than 300 journal articles and books, including four advanced research monographs: *Methods in Nonlinear Plasma Theory* (New York: Academic, 1972), *Theory of Nonneutral Plasmas* (New York: Benjamin, 1974), *Physics of Nonneutral Plasmas* (Reading, MA: Addison-Wesley, 1990), and *Physics of Intense Charged Particle Beams in High Energy Accellerators,* with H. Qin (Singapore: World Scientific, 2001). During 1976–1978 he served as Assistant Director for Applied Plasma Physics, Office of Fusion Energy, Department of Energy. He also served as Director of the MIT Plasma Fusion Center from 1978–1988, as the first Chairman of the DOE Magnetic Fusion Advisory Committee (MFAC) from 1982–1986, as Chair of the American Physical Society's Division of Plasma Physics during 1983–1984 and Division of Physics of Beams during 2001–2002, and has participated in numerous national and international committees on plasma physics and fusion research.

Dr. Davidson is a Fellow of the American Physical Society, a Fellow of the American Association for the Advancement of Science, and a member of Sigma Xi. He is also a recipient of the Department of Energy's Distinguished Associate Award and the Fusion Power Associates Leadership Award, both in 1986, and recipient of The Kaul Foundation's Award for Excellence in Plasma Physics Research in 1993.